

Cold gas dynamic spraying (CGDS) of TiO₂ (anatase) powders onto poly(sulfone) substrates: Microstructural characterisation and photocatalytic efficiency

I. Burlacov^a, J. Jirkovský^b, L. Kavan^b, R. Ballhorn^c, R.B. Heimann^{d,*}

^a Infineon Technologies Dresden, Königsbrücker Str. 180, D-01099 Dresden, Germany

^b J. Heyrovský Institute of Physical Chemistry, Academy of Sciences of the Czech Republic, Dolejškova 3, CZ-182 23 Prague 8, Czech Republic

^c IGGB Ingenieurbüro, Büschelstrasse 11, D-64297 Darmstadt, Germany

^d Oceagate Consulting GbR, Questenbergweg 48, D-34346 Hann. Münden, Germany

Received 26 July 2006; received in revised form 15 October 2006; accepted 26 October 2006
Available online 3 November 2006

Abstract

Thin TiO₂ coatings were deposited by cold gas dynamic spraying (CGDS) on different types of thermoplastic poly(sulfone) material using nitrogen as process gas and commercially available TiO₂ (anatase) powder as feedstock. The properties of the coatings were investigated as functions of gas temperature and pressure. Coating microstructure and phase composition were characterised by scanning electron microscopy and micro-Raman spectroscopy, respectively. The photocatalytic efficiency of the coatings was monitored through the decomposition of 4-chlorophenol in aqueous solution, and the initial reaction rates, *i.e.* rates of pH decrease compared to those of standard Degussa P-25 coatings. It was found that most CGDS coatings showed excellent adhesion to the substrate and suitable surface roughness as well as photocatalytic activities equal to or higher than those of the reference coating.

© 2006 Elsevier B.V. All rights reserved.

Keywords: Titania (anatase) coatings; Poly(sulfone)s; Cold gas dynamic spraying (CGDS); Raman spectroscopy; Photocatalytic activity

1. Introduction

The outstanding photocatalytic activity of the anatase polymorph of titanium dioxide (TiO₂) [1] has led to the design and development of many new effective reactors for purification of industrial and domestic wastewater and gasses. Since immobilisation of TiO₂ photocatalyst in the form of a coating has many practical advantages over suspended powder, in the past various coating techniques including thermal spraying [2–4], chemical vapour deposition [5] and, in particular sol–gel deposition [6] have been tested to produce well-adhering coatings with favourable surface properties. However, to achieve mechanical stability of sol–gel derived TiO₂ coatings and high crystallinity during its subsequent calcination treatment, high temperatures in the range of 450–750 °C must still be applied.

This has dramatic consequences since at elevated temperature an irreversible polymorphic transformation occurs of the anatase phase to the photocatalytically less active rutile phase. Hence there is a necessity to process TiO₂ (anatase) coatings at temperatures substantially below the onset of phase transition to rutile. Cold gas dynamic spray (CGDS) deposition appears to be a convenient technology to achieve this goal.

The decisive advantage of CGDS over competing conventional techniques is its low deposition temperature in conjunction with high pressure of the carrier gas that imparts high kinetic energy to the solid powder particles. Most ductile metals such as Cu, Al, Ni, Ti and Ni-based alloys can be deposited by cold gas dynamic spraying, and even ceramics and polymers [7] can be embedded into a substrate surface to form a thin coating layer.

The CGDS technique was invented by Papyrin and coworkers in Russia [8] and has been subject to intense industrial interest ever since [9,10]. The advantages of the technique include low temperature powder processing, phase preservation, very

* Corresponding author. Tel.: +49 5541 903073; fax: +49 5541 903181.
E-mail address: robert.heimann@ocean-gate.de (R.B. Heimann).

little oxidation of powder, coating and substrate, high coating hardness due to formation of a cold-worked microstructure, elimination of solidification stresses and hence possibility to deposit thicker coatings, coatings with low defect density, low heat input into the substrate hence reduced cooling requirements, as well as reduced or even eliminated need for fuel gasses, electrical heating and sample masking. However there are also some noticeable disadvantages including high gas flow rates of costly gasses such as helium required to achieve maximum particle velocity, limitation of coating materials to ductile metallic powders, and the fact that the technology is still mainly in its research and development stage with little coating performance and history data.

The mechanism of bonding of the coating layer to the substrates relies on sufficient energy to cause significant plastic deformation of the particle and the substrate as well (“micro-forging”). Under high impact stresses and strains interaction of the particle with the substrate surface presumably causes a disruption of oxide films thus promoting contact of chemically clean surfaces. In addition, high friction will generate very high-localised temperatures that will result in bonding akin to explosive welding.

Ceramic powder particles such as TiO₂ should reach even higher velocities compared to metallic powder because of their lower densities and inertia. The particle velocity will also be influenced by the size and geometric shape of the particles, their grain size distribution, the type and dynamic properties of the accelerating gas (density, ratio c_p/c_v) and the drag coefficient C_D [11]. In addition the velocity of the particle will be determined by the operating pressure and temperature of the gas, and the nozzle design (Mach number). However, cold spraying of ceramic [12] and polymeric [7] particles is still a controversial issue as the bonding mechanism is associated to permanent high-rate deformation at the particle-substrate interface, typical of metallic behaviour. Also, owing to their lower inertia ceramic particles suffer much more from bow shock deceleration prior to impact compared to metal particles.

The materials limitation notwithstanding early attempts were reported in the literature to deposit ceramic coatings by CGDS. In particular, Li et al. [12,13] described the deposition of titania powder by CGDS onto stainless steel substrates. The coating thickness was limited to below 15 μm , and its high porosity and

discontinuous nature did not allow to use the UV light applied to its most efficient degree, hence reducing the photocatalytic performance of the coating. Obviously the brittle, non-ductile nature of the titania powder led to increased surface erosion so that attempts to deposit thicker, continuous coatings were thwarted.

Hence it was thought that a soft substrate provided by a polymeric surface would allow to anchor the highly accelerated hard and brittle titania particles solidly within surface asperities produced by impact with high kinetic energy. Since some thermoplastic polymers exhibit properties conducive to the utilisation in photocatalytic reactors such a light weight, reasonable transmissivity in the UV–vis–NIR, mechanical flexibility, reasonable chemical stability against UV-A radiation, cost efficiency, and generally well-known processability, the combination of a homogeneous, thin, well-adhering titania (anatase) coating deposited by CGDS with a polymer substrate with satisfactory UV transmittance, and mechanical and chemical stability could potentially provide a paradigm shift for liquid and gaseous waste treatment by photocatalysis. Results of these attempts reported in this contribution are in the process of being protected by patent law [14].

2. Materials and methods

2.1. Materials

2.1.1. Substrates

Different types of thermoplastics sheet (143 mm \times 143 mm \times 2 mm) were tested as substrates for CGDS coatings including poly(etheretherketone) (PEEK), poly(ethyleneterephthalate) (PET), poly(vinylidene fluoride) (PVDF), poly(sulfone) (PSU), poly(ethersulfone) (PES) and poly(phenylsulfone) (PPSU). Based on evaluation of their thermal stability during the CGDS coating process (Table 1), transmittance in the UV range, water and water vapour absorption, chemical resistance, processability, and cost efficiency three types of thermoplastic material of the poly(sulfone) family were selected as substrates for titania coatings. These polymers included PSU (tradename UdelTM), PES (tradename Radel-ATM) and PPSU (tradename Radel-RTM) materials supplied by Solvay Advanced Polymers L.L.C.

Table 1
Densities and thermal properties of thermoplastics used as substrates

Material	Supplier	Heat resistance and melting point			
		Density (g/cm ³)	Short time heat stability (°C)	Long time heat stability ^a (°C)	Melting point (°C)
PEEK	Reiff GmbH	1.31	310	250	340
PET		1.39	160	115	255
PVDF		1.79	160	150	175
PSU (Udel TM)	Solvay Advanced Polymers L.L.C.	1.24	n/a	174	185 ^b
PES (Radel A TM)		1.37	n/a	204	n/a
PPSU (Radel-R TM)		1.29	n/a	205	220 ^b

^a Heat deflection temperature (HDT).

^b Glass transition temperature T_g .

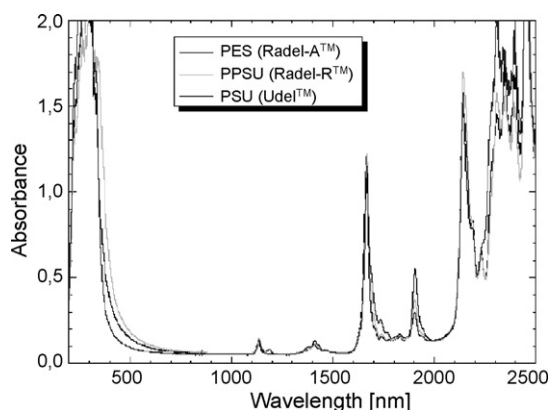


Fig. 1. UV-vis-NIR absorption spectra of the poly(sulfone)s UdelTM, Radel-ATM and Radel-RTM.

Fig. 1 shows the absorbance spectra in the wavelength range between 200 and 2500 nm of the poly(sulfone)s PSU (UdelTM), PES (Radel-ATM) and PPSU (Radel-RTM). The spectra are very similar; in particular, transmission of electromagnetic radiation with wavelengths between 400 nm and about 1600 nm is very high thus suggesting suitable optical properties for the envisaged application of the three selected poly(sulfone)s as carriers of photocatalytically active titania coatings.

2.1.2. TiO₂ powder

A commercially available agglomerated TiO₂ (anatase) powder (tradename HombikatTM TS-40; Sachtleben Chemie GmbH, Duisburg, Germany) with a primary particle size of <10 nm and an agglomerated particle size distribution of $Q_{.50} = 45 \mu\text{m}$ (median) and $Q_{.90} = 60 \mu\text{m}$ was used as feedstock.

2.2. Methods

2.2.1. Cold gas dynamic spraying (CGDS)

During cold gas spraying, very high particle velocities are obtained by acceleration of a gas stream expanding in a converging-diverging de Laval-type nozzle to velocities in the range of 300–1200 m/s. The length of the convergent nozzle section was 73 mm, the internal throat diameter was 2.7 mm, and the expansion ratio was about 9.7.

The schematics of the CGDS set-up is presented in Fig. 2. Next to gas pressure and temperature, the most important process parameter is the particle velocity prior to impact at the

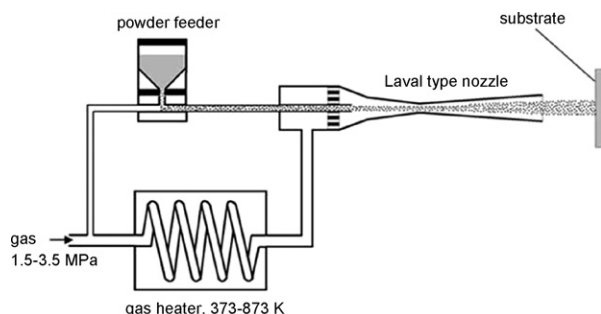


Fig. 2. Schematics of the set-up used for cold gas dynamic spraying [9].

Table 2
CGDS operating parameters

Type of carrier gas	Nitrogen
Powder type	Hombikat TM TS-40
Primary particle size	<10 nm
Median powder grain size	45 μm
Working gas pressure	1.5–3.0 MPa
Gas temperature at nozzle exit	400–550 °C
Particle velocity	900–1000 m/s
Powder feed rate	5–10 g/min
Stand-off distance	30 mm
Traverse speed of spray gun	80–100 mm/s
Number of traverses	1
Down-shift step of spray gun	1.5 mm

substrate. Since for any given material a critical particle velocity exists only those particles with a velocity exceeding this critical velocity can be deposited to produce a well-adhering coating. Particle with velocities below the critical velocity will only lead to erosion of the substrate. The critical particle velocities of Cu, Fe, Ni and Al are approximately 560–580, 620–640, 620–640 and 680–700 m/s, respectively [10]. However, since the critical velocity is a complex function of a number of variables published values are usually calculated ones and thus do not accurately reflect measured data. Since in the present case TiO₂ particle velocities could also not be measured reliably they were estimated to be between 900 and 1000 m/s using a one-dimensional isentropic equation [11].

2.2.2. Experimental parameters

Table 2 shows the deposition parameters applied using CGDS equipment (Kinetic 3000 Cold Spray System; CGT, Ampfing, Germany) operated at Freiburger NE-Metall GmbH & Co Produktion KG, Freiberg, Germany (Fig. 3). Coatings were obtained with only one pass of the spray torch to form deposits of about 20 μm thickness. The torch was moved in a meander-like fashion across the substrate surface with a downshift step of 1.5 mm.

2.2.3. Coating characterisation

The microstructure of the surfaces of as-sprayed TiO₂ coatings was characterised by optical microscopy at different magnifications. Cross-sections were coated with a thin layer of carbon and secondary electron images obtained by scanning electron microscopy (SEM JSM-6400) at 20 kV acceleration voltage and a beam current of 600 pA at the Department of Geology, Technische Universität Bergakademie Freiberg, Germany. The phase composition of the coatings was characterised by micro-Raman spectroscopy using a Jobin Yvon LabRam HR-800 spectrometer operated at the Department of Theoretical Physics, Technische Universität Bergakademie Freiberg, Germany. The 532 nm wavelength line of a Nd:YAG laser with an output power of 0.5–24 mW was used for excitation. Raman spectra were collected at 5, 10 and 50 times magnification in backscattering geometry. The spot size of the laser probe was between 2 and 10 μm . The spectral resolution was better than 1 cm^{-1} .

The surface roughness of the deposited coatings was measured using a UBM Surface Topography tester.



Fig. 3. Kinetic 3000 Cold Spray System operated at Freiburger NE-Metall GmbH & Co Produktion KG, Freiberg, Germany (left) and close-up view of the spray nozzle (right). Coated polymer samples are shown on the rack in the left image.

The photocatalytic activity of the coatings was tested in a mini-photoreactor based on a standard spectroscopic cell (Fig. 4) using the decomposition reaction of 10 mM 4-chlorophenol in 10 mM NaClO₄ aqueous solution [4].

The sample was irradiated by polychromatic UV light (>320 nm) generated by a mercury lamp (Narva HBO 200, 26 V, 2 A). The UV radiation was filtered with an IR liquid filter and with a 320 nm glass cut-off filter WG-3 (Saale-Glas GmbH, Jena, Germany). The pH change following the release of hydrochloric acid was continuously monitored by a glass electrode positioned above the coating sample. The initial reaction rate of the HCl formation is thought to be proportional to the photocatalytic activity of the coating. The kinetic parameters were determined from the dependence of pH on irradiation time. The initial rates of pH decrease ($-d(\text{pH})/dt$) obtained were compared with that of a standard Degussa P-25 coating measured under identical test conditions. A vitreous silica reference plate was coated with Degussa P-25 powder suspended in methanol and calcined at 650 °C for 2 h.

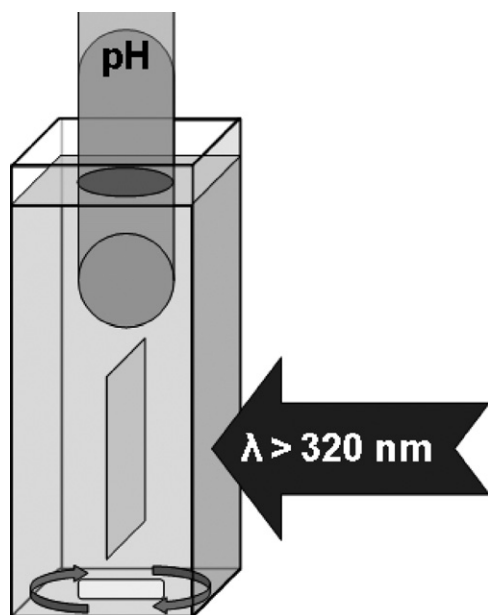


Fig. 4. Mini-photoreactor operated at the J. Heyrovský Institute of Physical Chemistry, Academy of Sciences of the Czech Republic, Prague, Czech Republic.

3. Results and discussion

3.1. Microstructure of coatings

Since all poly(sulfone) substrates are transparent in visible light (Fig. 1) the microstructures of the deposited coatings were investigated through the backside of the thin (2 mm) substrates. Fig. 5 shows that the highly accelerated TiO₂ particles impacting the substrate surface penetrated to a certain depth dependent on their kinetic energy and the elasticity of the thermally treated polymer. Comparison of the coatings produced at 450 °C (top row) and 500 °C (bottom row) reveals that the thermally less stable PES (panel B*) and PSU (panel C*) substrates softened considerably at higher gas temperature and hence allowed the TiO₂ to penetrate to larger depths forming particle clusters in contrast to the thermally more stable PPSU (panels A and A*). Darker spots visible in panels B* and C* indicate overheated and thus locally melted parts of the polymer substrates.

Fig. 6, left shows an SEM micrograph of a cross-section of a poly(sulfone) (PSU, UdelTM) substrate coated with a TiO₂ layer of about 20 μm thickness, comparable to the results obtained previously [12]. Since ceramic particles are brittle and thus do not possess ductility as metal particles do they tend to erode on impact previously deposited material. Consequently only one traverse of the torch was used limiting the coating thickness achievable. Polymeric material squeezed out of the surface after particle impact will likely act as particle binder as shown in Fig. 6, right. This dislodged material may even cover parts of the topmost TiO₂ particle layer thus reducing together with sublimated and recondensed material (see below, Figs. 7 and 8) the photocatalytic efficiency of the anatase coating.

The roughness of the CGDS coatings is a very important quality parameter that controls the effective surface area and hence the efficacy of the photocatalytic performance of the TiO₂ coatings. Table 3 shows the surface roughness data R_a (arithmetic average roughness) and R_y (maximum profile depth) of uncoated poly(sulfone) and TiO₂ coatings deposited at 450 and 500 °C. While the roughness increases with increasing gas temperature it appears to be independent of the gas pressure at given temperature. The type of polymer has also no influence on the roughness of uncoated substrates.

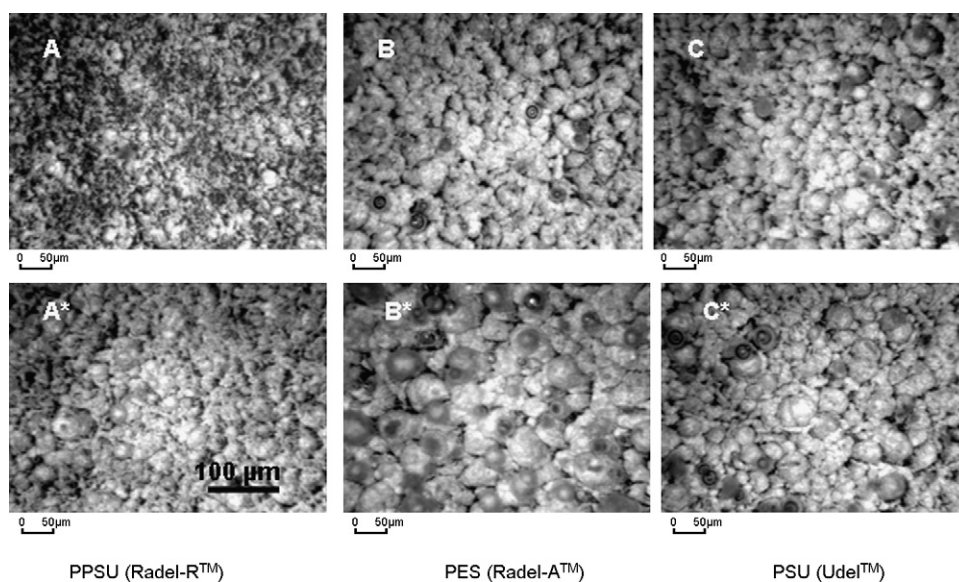


Fig. 5. Optical micrographs of TiO₂ coatings deposited by CGDS on several poly(sulfone) substrates at 450 °C, 30 bar nitrogen gas pressure (top row: A–C) and 500 °C, 30 bar nitrogen gas pressure (bottom row: A*–C*). Direction of view through the 2 mm thick polymer substrate accounts for the somewhat defocused appearance of the micrographs due to light scatter.

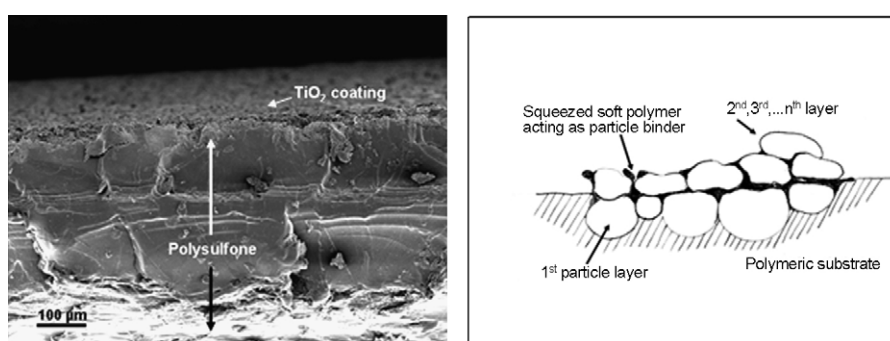


Fig. 6. Left: SEM micrograph showing an oblique view of a cross-section of PSU (bottom) coated with TiO₂ (top). Right: model of particle bonding of a CGDS coating on a polymer surface.

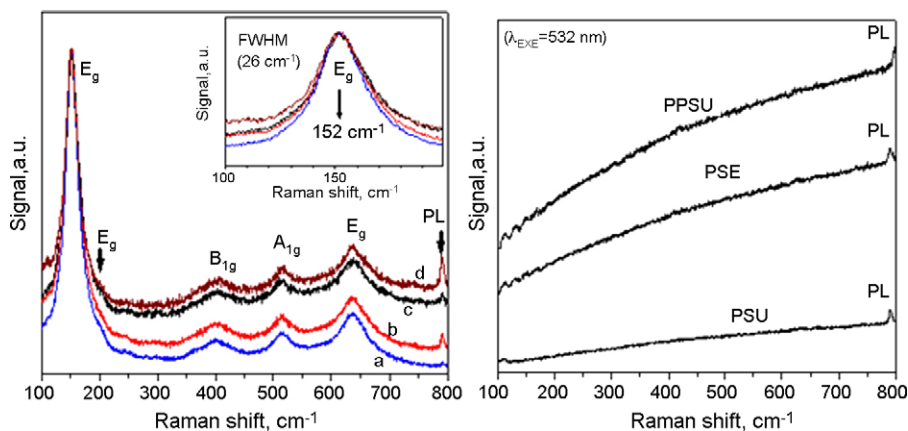


Fig. 7. Left: Raman spectra of PSU (Udel™) surfaces coated with TiO₂ (anatase) under different CGDS conditions. (a) 450 °C, 30 bar; (b) 450 °C, 20 bar; (c) 450 °C, 15 bar; (d) 500 °C, 30 bar. The inset shows the peak position and the change of the FWHM of the lowest E_g Raman mode. The peaks marked with an arrow (PL) indicate the presence of polymer (see text). Right: background Raman luminescence spectra of the three types of poly(sulfone) used (PSU, PES, PPSU) [14]. The peak at 790 cm⁻¹ marked with PL is the photoluminescence band characteristic for all poly(sulfone)s [17].

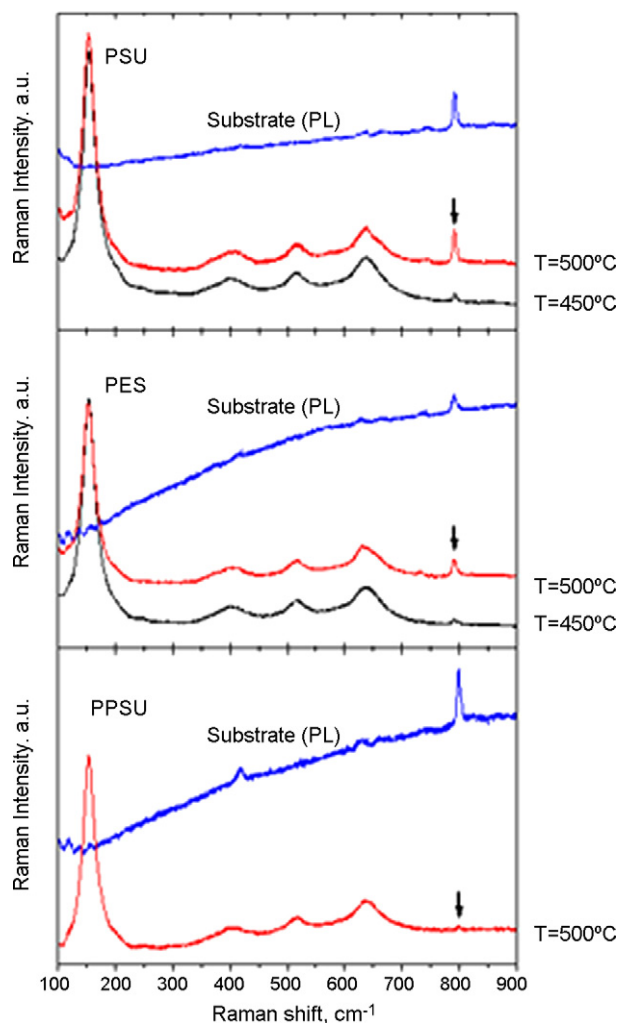


Fig. 8. Raman spectra of the surfaces of TiO₂ (anatase) coated poly(sulfone)s. The laser beam ($\lambda = 532$ nm) was focused on a 1–2 μm spot. The peaks marked by an arrow indicate the presence of contaminating polymer on top of the coating.

3.2. Phase composition

Owing to the rather low temperature exposure of the TiO₂ (anatase) particles during CGDS processing the phase composition of the starting powder could be completely preserved as confirmed by Raman spectroscopy. Fig. 7, left shows Raman spectra of coatings deposited on PSU (UdelTM) surfaces under various conditions (a: 450 °C, 30 bar; b: 450 °C, 20 bar; c: 450 °C, 15 bar; d: 500 °C, 30 bar) [14]. The typical Raman spectrum of anatase is composed of five characteristic Raman bands at 152(E_g), 197(E_g), 396(B_{1g}), 515(A_{1g}) and 638(E_g) cm^{-1} , corresponding to different vibration modes of the anatase structure

Table 3
Roughness parameters R_a and R_y of uncoated and CGDS TiO₂-coated substrates

Surfaces	R_a (μm)	R_y (μm)
Uncoated	0.09 ± 0.01	1.33 ± 0.57
Coated at 450 °C	1.76 ± 0.27^a	17.33 ± 3.63
Coated at 500 °C	3.36 ± 0.21	28.14 ± 0.76

^a Average of coatings obtained with gas pressures of 15, 20 and 30 bar.

for which the first E_g band at 152 cm^{-1} serves as an analytical fingerprint. Its blue shift from 144 cm^{-1} typically observed in bulk samples, and associated line broadening from about 8 to 26 cm^{-1} FWHM is related to phonon confinement that increases dramatically for crystallite sizes below 10 nm [15,16].

Fig. 7, right shows background photoluminescence spectra of the three polymer substrates used. The luminescence intensities correspond to the colour of the polymer material, *i.e.* the most transparent PSU (UdelTM) shows much lower background luminescence compared to the amber coloured PPSU (Radel-RTM). The sharp PL band at 790 cm^{-1} is close to the out-of-plane benzene ring C–H deformation at 788.1 cm^{-1} [16], and its presence in the integrated spectra (Fig. 7, left) allows to estimate some deposition quality indicators such as coating continuity, homogeneity, and thickness. As shown in Fig. 7, left in the spectra a to c the PL band has a low intensity that increases for sample d, *i.e.* a TiO₂ coating deposited at higher temperature. This suggests that in the latter case the coating has become contaminated with polymer material sublimated from the substrate surface during thermal impact of the hot carrier gas and subsequent condensation on top of the as-deposited coating (cp. Fig. 6, right). This will significantly reduce the effective surface area of the TiO₂ coating and hence compromise its photocatalytic performance. Consequently the higher the temperature stability of the polymer substrate the lower is the risk of contamination at any given deposition temperature.

Fig. 8 shows that for PSU (UdelTM) with a rather low thermal stability (Table 1) the effect of self-contamination is much higher than for the thermally more stable PES (Radel-ATM) and, most notable, PPSU (Radel-RTM) as shown by the close to negligible intensity of the PL band in the Raman spectrum of the latter even at 500 °C gas temperature. In addition the spectra show that increasing the gas temperature from 450 to 500 °C also increases the intensity of the PL peak. This essentially means that for improvement of coating performance the thermal impact, *i.e.* the cumulative effect of gas temperature, gas pressure and stand-off distance has to be adjusted for each substrate material used by defining a balance between the kinetic energy of the accelerated powder particles and the mechanical properties of the substrate that will become thermoplastically pliable and mobilised by interaction with the hot gas stream.

3.3. Photocatalytic performance

The photocatalytic degradation of 4-chlorophenol on contact with a UV-irradiated TiO₂ (anatase) coating was found to proceed according to a first-order kinetics law [18]. Since the concentration of protons released during photodegradation increases exponentially with irradiation time, the pH, *i.e.* the negative logarithm of the proton concentration ought to decrease linearly. However, as shown in Fig. 9, left this is seemingly not the case. The reason for this deviation from theory can be tentatively seen in two facts. First, according to the classic Nernst law the electrochemical potentials of the photogenerated charges, *i.e.* electrons and holes depend on pH, *i.e.* they become more negative with increasing pH or more positive with

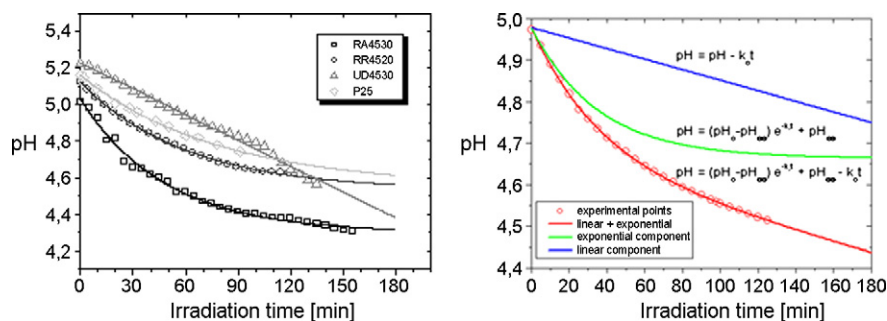


Fig. 9. Left: decrease of pH of 10 mM 4-chlorophenol in 10 mM NaClO_4 aqueous solution with irradiation time for selected anatase coatings (for explanation of labels cp. Fig. 10). Right: formal deconvolution of a measured pH vs. t curve into a linear contribution ($pH = pH_0 - k_0 t$) and an exponential contribution ($pH = (pH_0 - pH_\infty) \exp(-k_1 t) + pH_\infty$) with $pH_0 = (2.489 \pm 9.39) \times 10^{-4}$, $pH_\infty = 2.174 \pm 0.012$, $k_0 = (0.00127 \pm 9.882) \times 10^{-5}$, and $k_1 = 0.02816 \pm 0.0013$.

decreasing pH. Consequently during the one-electron oxidation of 4-chlorophenol the process accelerates with decreasing pH and, at the same time, the one-electron reduction process of molecular oxygen slows down.

However, even though the two processes occur separately but not independently on the TiO_2 particle surfaces, they are both required to close the photocatalytic loop and hence depend on each other. The overall reaction rate of the degradation of 4-chlorophenol is then determined by the rate-determining reaction step, *i.e.* the slower one and as a result it depends less on pH than on the conditions given by the particular redox process. This may impose a non-linearity on the overall process as shown in Fig. 9, left.

As this effect is presumably rather small for small changes of the pH another explanation for the non-linear behaviour of the pH was considered. It was observed in a blank experiment, *i.e.* during UV irradiation of a TiO_2 coating on a poly(sulfone) substrate in the absence of 4-chlorophenol that a similar non-linearity exists. On the other hand, comparable coatings deposited on titanium substrates showed no pH change upon irradiation in the absence of 4-chlorophenol but the expected strictly linear response during photodegradation of 4-chlorophenol instead [4]. This suggests that the nature of the substrate has a decisive effect on the pH evolution in that UV-generated partial destruction of the poly(sulfone) chains may produce relatively strong organic or even sulfuric acids whose effect produce the non-linear kinetics observed. However, while the reaction rate of the decomposition of 4-chlorophenol remains constant that of acidity generated by degradation of the polymers slows down during the measuring period. This is shown in Fig. 9, right for a coated Radel-ATM substrate (gas temperature 450 °C, gas pressure 15 bar). The curves of measured pH versus irradiation time can formally be deconvoluted into a linear ($pH = pH_0 - k_0 \cdot t$) and an exponential contribution ($pH = (pH_0 - pH_\infty) \exp(-k_1 t) + pH_\infty$). Hence to compare the photocatalytic efficiency of TiO_2 coatings on poly(sulfone) substrates deposited at various gas temperatures and pressures an additive fitting function $pH = (pH_0 - pH_\infty) \exp(-k_1 t) + pH_\infty - k_0 t$ was applied. The fitting parameters pH_0 (pH at $t=0$), pH_∞ (pH at $t=\infty$) and k_1 and k_0 were then used to calculate the initial reaction rates, *i.e.* the change of pH as a function of the reaction time $(-d(pH)/dt)_0 = -k_1(pH_0 - pH_\infty) - k_0$ as shown in Fig. 10.

The initial reaction rates were compared to the reaction rate obtained for photodegradation of 4-chlorophenol on standard Degussa P-25 immobilised on a vitreous silica plate (dashed line in Fig. 10). The photocatalytic performances of most CGDS coatings compared favourably to that of P-25 coating, and maximum degradation rates were obtained for TiO_2 (anatase) coatings deposited on poly(ethersulfone) (Radel-ATM) plates at a gas temperature of 450 °C and pressures of 20 or 30 bar. Lower gas pressure (15 bar) or high gas temperature (500 °C) yielded reduced photocatalytic efficiencies presumably owing to respectively, reduced adhesion of the coating particles and shielding by self-contamination with sublimated polymer as discussed above. Moreover, the reaction rates of TiO_2 coatings on poly(phenylsulfone) (PPSU, Radel-RTM) are substantially below those on poly(ethersulfone) (PES, Radel-ATM). This may be related to the higher hardness of PPSU resulting in reduced deformation on particle impact and hence build-up of a thinner and in part non-continuous TiO_2 coating layer with less active surface area (cp. Fig. 5A and A*). On the other hand, the comparatively low photocatalytic activity of TiO_2 -coated PSU (UdelTM) surfaces is presumably related to the high degree of self-contamination of the thermally less stable polymer that led to shielding of the photocatalytically active surface area (cp.

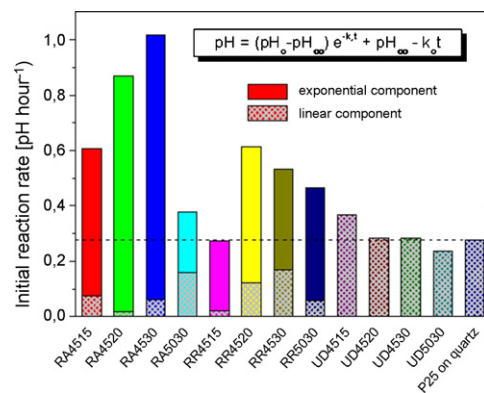


Fig. 10. Initial reaction rates during decomposition of 4-chlorophenol on CGDS titania coatings immobilised on PES (Radel-ATM), PPSU (Radel-RTM) and PSU (UdelTM) surfaces. The separation into linear and exponential contributions is shown. The bar labels characterise the type of substrate (RA = PES, RR = PPSU, UD = PSU), the gas temperature (45 = 450 °C, 50 = 500 °C) and the gas pressure (15, 20 and 30 bar).

Fig. 8). It was observed that the drop of pH on coated Udel™ substrates is linearly related to the irradiation time as opposed to Radel-A™ and Radel-R™ (Fig. 9, left) possibly suggesting improved stability against UV radiation of the former. It should be emphasised that the kinetic function applied above describes only formally the pH dependency on irradiation time but does not allow any interpretation of the real processes occurring at the contact interface anatase–polymer.

4. Conclusion

TiO₂ coatings with anatase structure were deposited by cold gas dynamic spraying (CGDS) on three different poly(sulfone) substrates, *i.e.* poly(sulfone) PSU (Udel™), poly(ethersulfone) PES (Radel-A™) and poly(phenylsulfone) PPSU (Radel-R™) at 450 and 500 °C gas temperature, and 15–30 bar nitrogen gas pressure. Raman spectroscopy confirmed that the phase composition of the precursor TiO₂ powder was conserved during the deposition process. The coatings showed superior adhesion to the polymeric substrates, surface roughness *R_a* values between 1.8 μm (450 °C) and 3.4 μm (500 °C), and photocatalytic efficiencies equal to or higher than that of the reference coating Degussa P-25. In particular, coatings deposited on PES (450 °C, 20–30 bar) showed initial reaction rates (rate of pH decrease) between 0.6 and 1.0 pH/h, whereas those deposited at comparable conditions on PPSU and PSU showed values of 0.3–0.6 and 0.25–0.40 pH/h, respectively. The initial reaction rate of the control (standard Degussa P-25 coating) was about 0.29 pH/h.

It was found that at higher gas temperatures the polymer surfaces partly underwent thermally induced sublimation and that the mobilised material showed a tendency to become redeposited on top of the TiO₂ particles thus reducing their photocatalytic efficiency. This problem of self-contamination may be overcome by either applying lower gas temperatures or depositing a very thin chemical barrier coating on the polymer surface [14] prior to CGDS of titania.

Acknowledgements

The work described in this contribution was sponsored by the Commission of the European Community, EC FP5 “Growth”

Programme CRAFT Project on “Innovative Thin-Film UV-Reactor (UVREC)”, contract EVKI-2002-30025 and by the Czech Ministry of Education, Youth and Sports through COST D35 Action 1P05OC069 and COST OC104 Action 540. Dr. Steffen Marx, Freiburger NE-Metall GmbH & Co Produktion KG, Freiberg, Germany is gratefully acknowledged for providing the CGDS coatings as a subcontractor.

References

- [1] A. Fujishima, K. Honda, *Nature* 238 (1972) 37.
- [2] F.X. Ye, A. Ohmori, C.J. Lee, in: C. Moreau, B. Marple (Eds.), *Thermal Spray 2003: Advancing the Science & Applying the Technology*, ASM International, Materials Park, OH, USA, 2003, p. 169.
- [3] N. Berger-Keller, D. Bertrand, C. Coddet, C. Meunier, in: C. Moreau, B. Marple (Eds.), *Thermal Spray 2003: Advancing the Science & Applying the Technology*, ASM International, Materials Park, OH, USA, 2003, p. 1403.
- [4] I. Burlacov, J. Jirkovský, M. Müller, R.B. Heimann, *Surf. Coat. Technol.* 201 (2006) 255.
- [5] S.A. O’Neill, R.J.H. Clark, I.P. Parkin, *Chem. Mater.* 15 (2003) 46.
- [6] M.Z. Atashbar, H.T. Sun, B. Gong, W. Wlodarski, R. Lamb, *Thin Solid Films* 326 (1998) 238.
- [7] Y. Xu, I.M. Hutchings, *Surf. Coat. Technol.* 201 (6) (2006) 3044.
- [8] P. Alkhimov, A.N. Papyrin, V.P. Kosarev, N.J. Nesterovich, M.M. Shuspanov, *Gas-dynamic spraying method for applying a coating*, US Patent 5,302,414 (April 12, 1994).
- [9] J. Voyer, T. Stoltenhoff, H. Kreye, in: C. Moreau, B. Marple (Eds.), *Thermal Spray 2003: Advancing the Science & Applying the Technology*, ASM International, Materials Park, OH, USA, 2003, p. 71.
- [10] F. Gärtner, T. Stoltenhoff, T. Schmidt, H. Kreye, *J. Therm. Spray Technol.* 15 (2) (2006) 223.
- [11] F. Raletz, M. Vardelle, G. Ezo’o, *Surf. Coat. Technol.* 201 (2006) 1942.
- [12] C.J. Li, W.Y. Li, *Surf. Coat. Technol.* 167 (2003) 278.
- [13] C.J. Li, G.J. Yang, X.C. Huang, W.Y. Li, A. Ohmori, in: E. Lugscheider (Ed.), *Proceedings of the International Thermal Spray Conference (ITSC)*, Osaka, Japan, DVS-Verlag, 2004, p. 315.
- [14] Offenlegungsschrift DE 10 2004 038 795 A1 (Verfahren zur Herstellung photokatalytisch aktiver Polymere), Deutsches Patentamt, 2. März 2006.
- [15] W.F. Zhang, Y.L. He, M.S. Zhang, Z. Yin, Q. Chen, *J. Phys. D: Appl. Phys.* 33 (2000) 912.
- [16] T.D. Robert, L.D. Laude, V.M. Geskin, R. Lazzaroni, R. Gouttebaron, *Thin Solid Films* 440 (2003) 268.
- [17] H.J. Kim, A.E. Fonda, K. Jonasson, *J. Appl. Polym. Sci.* 75 (1) (2000) 135.
- [18] J. Krýsa, G. Waldner, H. Měšťánková, J. Jirkovský, G. Grabner, *Appl. Catal. B: Environ.* 64 (2006) 290.